ISSN 0036-0244, Russian Journal of Physical Chemistry A, 2017, Vol. 91, No. 12, pp. 2377–2382. © Pleiades Publishing, Ltd., 2017.
Original Russian Text © N.M. Berezina, M.I. Bazanov, A.A. Maksimova, A.S. Semeikin, 2017, published in Zhurnal Fizicheskoi Khimii, 2017, Vol. 91, No. 12, pp. 2084–2090.

PHYSICAL CHEMISTRY OF SOLUTIONS

Electrochemical Behavior of *meso*-Substituted Iron Porphyrins in Alkaline Aqueous Media

N. M. Berezina*, M. I. Bazanov, A. A. Maksimova, and A. S. Semeikin

Ivanovo State University of Chemistry and Technology, Ivanovo, 153000 Russia

**e-mail: sky_berezina@rambler.ru*

Received December 29, 2016

Abstract—The effect *meso*-substitution in iron porphyrin complexes has on their redox behavior in alkaline aqueous solutions is studied via cyclic voltammetry. The voltammetric features of the reduction of iron pyridylporphyrins suggest that the sites of electron transfer lie at the ligand, the metal ion, and the pyridyl moieties. The electron transfer reactions between the different forms of these compounds, including the oxygen reduction reaction they mediate, are outlined to show the sequence and potential ranges in which they occur in alkaline aqueous media. Under our experimental conditions, the iron porphyrins exist as μ-oxo dimmers whose activity for the electrocatalytic reduction of oxygen displays a considerable dependence on the nature of the substitutents and nitrogen isomerization (for pyridylporphyrins) and grows in the order $(Fe(ms\text{-}Ph)_4P)_2O$, $(Fe[ms\text{-}(Py\text{-}3)Ph_3]P)_2O$, $(Fe[ms\text{-}(Py\text{-}4)_4]P)_2O$, and $(Fe[ms\text{-}(Py\text{-}3)_4]P)_2O$.

Keywords: meso-substituted porphyrins, iron complexes, electrochemistry, cyclic voltammetry, electrocatalysis, dioxygen

DOI: 10.1134/S0036024417120032

INTRODUCTION

Porphyrins are known for the diversity of beneficial properties that can be exploited [1]. Due to the established importance of metal porphyrins in biological, biocatalytic, and photocatalytic processes, they hold great potential for application in biology and medicine [2]. Almost limitless possibilities for modifying their core structures makes representatives of this class of compounds highly promising candidates for catalysis of the oxygen reduction reaction (ORR) in chemical power supplies [3–5].

All metal porphyrins are redox-active compounds. A given metal porphyrin is subject to a number of electron transfer processes, depending on several factors: the working range of potentials; the solvent that is used; the nature of the porphyrin macrocycle, the central metal ion(s), and the axial ligand(s) [6].

The electroreduction or electrooxidation of metal porphyrins is not always reversible; this depends on the experimental conditions of the electron transfer reaction. A redox process can proceed on the central ion(s) (metal-centered) or involve the π-conjugated system of the porphyrin rings (ring-centered). In some instances, extraligands and substituents associated with the porphyrin macrocycle can be subject to redox transformations as well [7–9].

Shown below is the scheme of electron transfer pathways [10] possible for the metal porphyrin that is the closest structural analog (with no extraligands) of the compounds studied in this work, their general formula being $[(P)Fe^{III}]^+$. Highlighted are two redox reactions involving the four molecular entities likely to form from the parental porphyrin: two π-cation radicals containing Fe(III) or Fe(IV) and two π-anion radicals containing Fe(I) or Fe(II). Most synthetic iron porphyrins are capable of causing three- or four-electron transfer reactions in non-aqueous media for $[(P)FeIII]^+$ [10]:

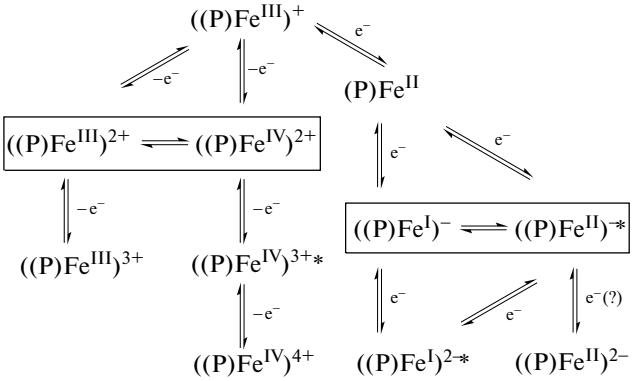

Even though the effect the nature of peripheral substituents in a porphyrin ring has on the redox behavior of substituted porphyrins has been the subject of numerous studies [8, 9, 11–14], a clear picture of this relationship has yet to be established. The presence of

electron-donating substituents in the porphyrin macrocycle usually favors oxidation and hampers the reduction of the π-conjugated system; the picture is reversed when electron-acceptor groups are present [10].

Tetra-substituted pyridylporphyrins and their complexes with Co(II), Cu(II), and Zn(II) can undergo redox reactions in aqueous alkaline media; these involve not only the metal centers (when present) and/or the π-conjugated system of the macrocycle, but also electron-acceptor substituents (e.g., pyridyl moieties), which reduce in the potential range of −0.7 to −0.8 V [15]. The redox behavior of active pyridyl substituents depends on the nature of the porphyrin macrocycle or, to be more exact, on the distribution of the electron density on the porphyrin molecule, which can act as a ligand or form a complex [15, 16].

Complexes whose porphyrin macrocycles have all meso positions substituted with pyridil moieties differ markedly from those with tetraphenylporphyrins as ligands, their nearest structural analogs, in both electrochemical behavior and electrocatalytic activity for the oxygen reduction reaction (ORR) [17].

In this work, which is a continuation of [15, 18, 19], we evaluate via cyclic voltammetry the effects that different substituents in a porphyrin ring have on the redox behavior of the respective iron porphyrins, and test the prepared compounds for activity in the ORR under electrochemical settings. Specifically, we consider the effects induced by C_6H_5- and C_5H_4N-substituents in *meso*-positions, and for pyridyl-substituted compounds we vary the position of the heteroatom (3- and 4-positions) with respect to the position at which the pyridine moiety attaches to the porphyrin core (referred to below as nitrogen isomerization). We are interested in particular in the redox potentials of these compounds that are associated with charge transfer at the Fe(III) site and the π-system of a porphyrine core. The structural formulas of the resulting compounds are shown below [20]:

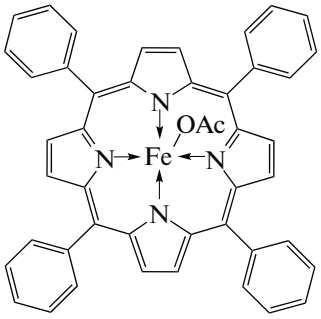

(OAc)Fe(*ms*-Ph)$_4$P

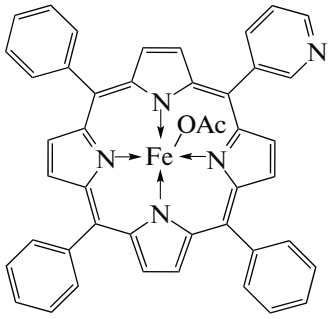

(OAc)Fe[*ms*-(Py-3)Ph$_3$]P

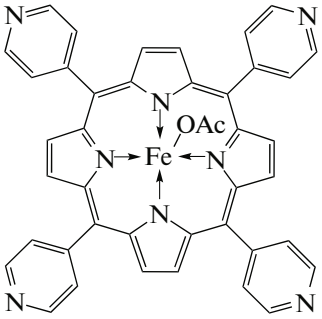

(OAc)Fe[*ms*-(Py-4)$_4$]P

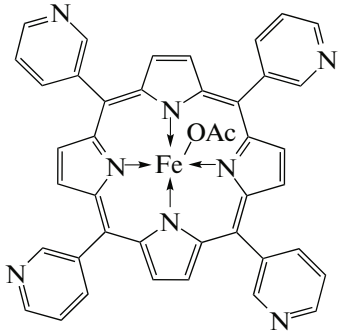

(OAc)Fe[*ms*-(Py-3)$_4$]P

EXPERIMENTAL

meso-Substituted porphyrin ligands were synthesized and purified as described in [21]. The synthesis of the respective iron porphyrins is described below.

We prepared 5,10,15,20-tetrakis(4-pyridyl)porphyrin iron (III) acetate ((OAc)(Fe[*ms*-(Py-4)$_4$]P)) by adding a tenfold excess of iron powder to a solution containing 50 mg (0.081 mmol) of the ligand (H_2T(Py-4)P) in 10 mL of acetic acid. The reaction mixture was refluxed for 2 h and then filtered once it was cooled. The filtrate was diluted with 20 mL of water and neutralized with aqueous ammonia, causing the target product to precipitate. This precipitate was collected by filtration and dissolved in chloroform, and the resulting chloroformic solution was purified via chromatography on alumina, with chloroform as

Table 1. Peak potentials and redox potentials (vs. Ag/AgCl) of the key processes that occurred on our porphyrin-modified electrodes; $v = 20$ mV s^{-1}

Porphyrin compound	$Fe^{3+} \leftrightarrow Fe^{2+}$ $Fe^{2+} \leftrightarrow Fe^{1+}$			Process I $L \leftrightarrow L^-$			Process II $L^- \leftrightarrow L^{2-}$ (Py)			Process III $L^- \leftrightarrow L^{2-}$, $L^{2-} \leftrightarrow L^{3-}$*		
	$-E_c$, V	$-E_a$, V	$-E_{redox}$, V	$-E_e^I$, V	$-E_a^I$, V	$-E_{redox}^I$, V	$-E_e^{II}$, V	$-E_a^{II}$, V	$-E_{redox}^{II}$, V	$-E_e^{II}$, V	$-E_a^{II}$, V	$-E_{redox}^{II}$, V
H_2(*ms*-Ph)$_4$P [17]	–	–	–	0.66	0.56	0.62	–	–	–	1.08	0.97	1.03
(Fe(*ms*-Ph)$_4$P)$_2$O	0.39	0.34	0.37	0.67	0.57	0.62	–	–	–	1.05	1.00	1.03
	1.40**	1.26**	1.33**									
Fe(*ms*-Ph$_4$Br$_8$P)$_2$O [22]	0.51	0.36	0.44	–	–	–	–	–	–	1.04	0.63	0.84
H_2(Py-4)$_4$P [15]	–	–	–	0.60	0.29	0.45	0.88	0.54	0.71	1.19*	–	1.12
(Fe[*ms*-(Py-4)$_4$]P)$_2$O	0.46	0.27	0.37	0.76	0.36	0.56	0.88	0.61	0.75	1.11*	–	–
H_2(Py-3)$_4$P [15]	–	–	–	0.61	0.48	0.54	0.81	0.61	0.71	1.06*	0.94	1.00
	$Fe^{3+} \rightarrow Fe^{2+}$/L $\rightarrow L^-$/$Fe^{2+} \rightarrow Fe^{1+}$**						$L^- \leftrightarrow L^{2-}$ (Py)			$L^{2-} \leftrightarrow L^{3-}$*		
(Fe[*ms*-(Py-3)$_4$]P)$_2$O	0.40		0.25		0.33		0.91	0.66	0.78	1.07	0.95	1.01
	1.34**		1.12**		1.23**							
(Fe[*ms*-(Py-3)Ph$_3$]P)$_2$O	0.46	0.33	0.49	0.61	0.34	0.48	–	–	–	1.14	0.62	0.88
	1.28**	–	–									

* Process $L^{2-} \leftrightarrow L^{3-}$ was observed only for pyridilporphyrins.
** $Fe^{2+} \rightarrow Fe^{1+}$ process.

an eluent (yield: 0.030 g (55%)). UV–Vis ($CHCl_3$; λ_{max} (nm), log ε): 415 (4.84); 508 (4.01); 660 (3.56).

The other two compounds—5-(pyridyl-3)-10,15,20-triphenylporphyrin iron (III) acetate ((OAc)[Fe[*ms*-(Py-3)Ph$_3$]P)) and 5,10,15,20-tetrakis(3-pyridyl)porphyrin iron (III) acetate (OAc)[Fe[*ms*-(Py-3)$_4$]P)—were synthesized in the same manner.

The purity of the prepared compounds was assessed, and their identity confirmed, via UV–Vis absorption spectroscopy on a SF-56 spectrophotomer and thin layer chromatography on Sulifol C60 plates using chloroform as an eluent.

Electrochemical characterizations via cyclic voltammetry (CV) were performed in a three-electrode cell (model YaSE-2) connected to a P-30J potentiostat. A graphite rod and a platinum plate served as the working and counter electrodes, respectively; potentials were recorded vs. a silver/silver chloride electrode. To test the electrochemical activity of the synthesized iron porphyrins, the surface of the working electrode (area, 0.64 cm^2) was covered with a layer of paste (0.2–0.3 mm thick) consisting of carbon black (type P-514, GOST 7885-86; ash content of 0.45%), a 6% suspension of FP-4D poly(tetrafluoroethylene) in alcohol, and one of the iron porphyrins in a mass ratio of 7 : 2 : 1, with ethanol as a liquid medium for the paste. Once the applied paste was dry, the electrode was briefly (for 1 min) annealed at 573 K.

For CV measurements, the working electrode, modified as described above with paste containing one of the investigated compounds (or with no paste for recording background CVs), was submersed in an electrolyte solution that was purged in advance with Ar (99.99%) for 40 min (rate of gas flow, 0.14 mL s^{-1}). The potential was scanned from 0.5 to −1.5 V and in the reverse direction. Once the measurements in argon were complete, dioxygen was introduced into the cell. Peak potentials on the CVs, which corresponded to charge transfer onto/from the test compounds, were accurately determined (±0.01 V) using dedicated software [18].

RESULTS AND DISCUSSION

Iron porphyrins display a considerable tendency to form μ-oxo bridged complexes, a characteristic feature of this type of compounds. Under the conditions of electrochemical measurements used in this work, the compounds of interest were in the form of μ-oxo dimmers, as was confirmed by the UV–Vis absorption data: (OAc)(Fe[*ms*-(Py-4)$_4$]P) [λ (nm), (log ε), $CHCl_3$]: 405 (4.74); 567 (3.77); 608 (3.55); (OAc)Fe[*ms*-(Py-3)$_4$]P: [λ (nm), (log ε), $CHCl_3$]: 410 (4.94); 570 (3.95); 610 (3.63); (OAc)Fe[*ms*-(Py-3)Ph$_3$]P: [λ (nm), (log ε), $CHCl_3$]: 410 (4.91); 570 (3.85); 611 (3.53).

Table 1 summarizes the key characteristics, extracted from the CV data, of the electrochemical

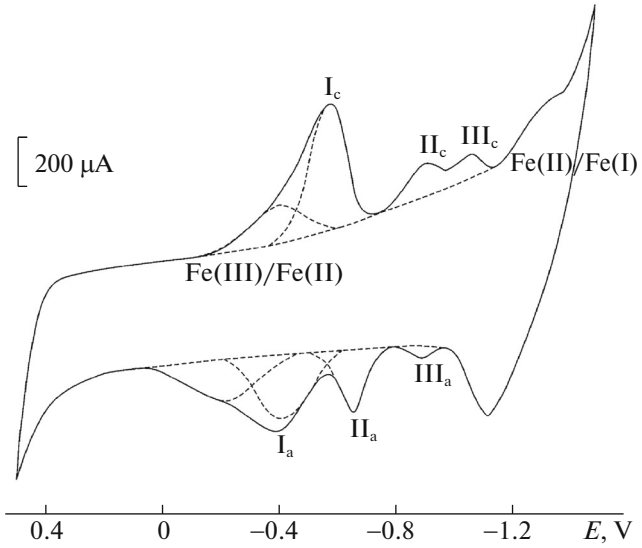

Fig. 1. CVs on the electrode modified with (Fe[*ms*-(Py-3)$_4$]P)$_2$O, at a scan rate of 20 mV s^{-1} under argon.

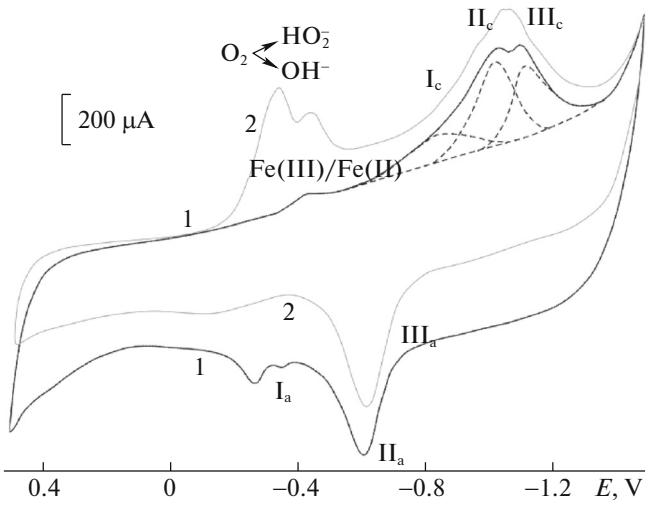

Fig. 2. CVs on the electrodes modified with (Fe[*ms*-(Py-4)$_4$]P)$_2$O in (*1*) a deaerated (Ar) soluton and (*2*) in an oxygen-saturated solution, at a scan rate of 20 mV s^{-1}.

processes (the peak potentials and formal potentials) that occurred on the graphite electrodes modified with either pure porphyrin ligands or iron porhyrin complexes as described above.

The electrochemical transformation of the ([Fe[*ms*-(Py-3)Ph$_3$]P)$_2$O, ([Fe[*ms*-(Py-4)$_4$]P)$_2$O, and ([Fe[*ms*-(Py-3)$_4$]P)$_2$O complexes under oxygen-free conditions involve the porphyrin macrocycle.

For tetraphenylporphyrins, e.g., H$_2$(*ms*-Ph)$_4$P, (Fe(*ms*-Ph)$_4$P)$_2$O, and (Fe(*ms*-Ph$_4$Br$_8$P)$_2$O), we and others (see Table 1) detected two reduction processes, centered at the π-conjugated system, with redox potentials at −0.62 and −1.03 V. This suggests that process I for pyridylporhyrins is associated with the transfer of one electron to yield the corresponding radical anion. For (Fe[*ms*-(Py-4)$_4$]P)$_2$O and (Fe[*ms*-(Py-3)$_4$]P)$_2$O, process II corresponds to the electroreduction of one of their pyridyl moieties with E_{redox} = −0.78 and −0.89 V, respectively, as can be seen from the CVs (Figs. 1−3). Process III is associated with transfer of a third electron onto the π-system of the macrocycle.

As for the studied tetraphenylporphyrines—(Fe(*ms*-Ph)$_4$P)$_2$O and Fe(*ms*-Ph$_4$Br$_8$P)$_2$O—only two ring-centered reductions were observed (Fig. 3), which is typical of processes in nonaqueous media.

For (Fe[*ms*-(Py-3)$_4$]P)$_2$O (pyridyl nitrogen at the 3-position), the broad reduction current peak at potentials of −0.2 to −0.6 V is likely to be an overlapping of two peaks originating from the reduction of the central ion ($Fe^{3+} \rightarrow Fe^{2+}$) and the tetrapyrrole macrocycle (I_c). The process with E_{redox} = −1.23 V could be associated with the transfer of the second electrode onto the central ion, $Fe^{2+} \rightarrow Fe^{1+}$.

(Fe(*ms*-Ph)$_4$P)$_2$O and (Fe[*ms*-(Py-3)Ph$_3$]P)$_2$O undergo metal-centered reduction: $Fe^{3+} \leftrightarrow Fe^{2+}$ and $Fe^{2+} \leftrightarrow Fe^{1+}$, as can be seen from the CVs in Figs. 1 and 3. We could not, however, observe the second reduction, $Fe^{2+} \leftrightarrow Fe^{1+}$, since the evolution of hydrogen commenced at potentials notably lower than we expected (Fig. 2).

Unfortunately, the redox potentials of the formation of the anion radical yielded very little information regarding the effect complexation and nitrogen isomerization have on the reduction of the tetrapyrrole ring; overlapping electron transfer processes in the case of (Fe[*ms*-(Py-3)$_4$]P)$_2$O reduction made analysis of the CV data even more complicated.

Apart from studying the electrochemical behavior of pyridyl-substituted porphyrins *per se*, we tested their performance as electrocatalysts for the ORR. When O_2 was introduced into the electrolytic cell, we detected a substantial increase in the current due to the oxygen reduction in the range of potentials from 0.0 to −0.4 V (Fig. 2, curve *2*).

Comparing the peak potentials and half-wave potentials ($E_{max}(O_2)$ and $E_{1/2}(O_2)$) for the tested compounds, we concluded that the iron porphyrins with pyridyl residues in all of the *meso*-positions substantially outperformed their counterparts with phenyl substituents in electrocatalytic activity (Table 2). In fact, both the nature and nitrogen isomerization (for pyridyl residues) of the *meso*-substituents determined the electrocatalytic activity of the investigated

complexes, which grew with the half-wave potential of the wave of oxygen reduction, $E_{1/2}(O_2)$, in the order $(Fe[ms\text{-}(Ph)_4]P)_2O$ < $(Fe[ms\text{-}(Py\text{-}3)Ph_3]P)_2O$ < $(Fe[ms\text{-}(Py\text{-}4)_4]P)_2O$ < $(Fe[ms\text{-}(Py\text{-}3)_4]P)_2O$. Parameters $E_{max}(O_2)$ and $E_{1/2}(O_2)$ broadly exhibit symbate variations with the nature of the complexes (Table 2).

In studying the effect scan rate v had on the electrocatalytic reduction of O_2, we determined that peak current I_{max} scaled linearly with $\sqrt{v}$. At the same time, the peak potential shifted cathodically, showing a linear dependency on the logarithm of the scan rate.

CONCLUSIONS

Our results support the possibility of porphyrins with electron withdrawing substituents (i.e., pyridyl residues) undergoing multielectron reduction in both pure (free) form and with coordinating iron atom(s). Our findings complement the redox transformations of the iron porphyrins by adding new redox reactions to the reaction diagram and specifying the sequence and ranges of potentials in which these reactions occur in alkaline aqueous media:

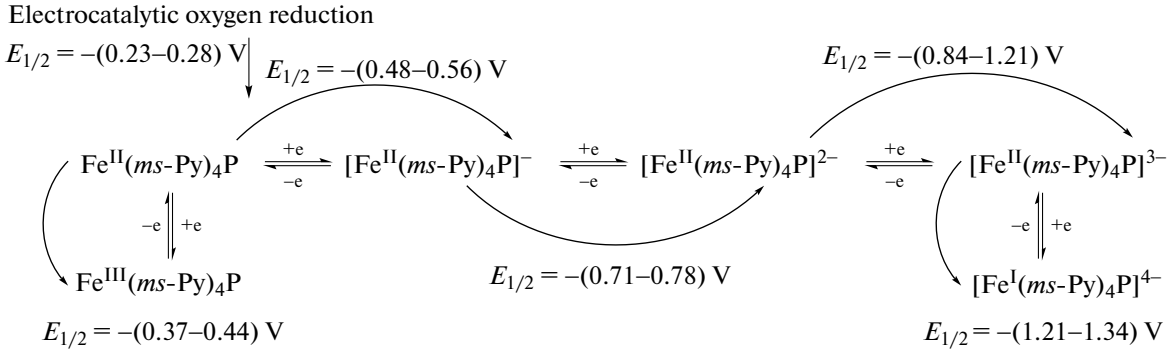

The diagram also specifies the place for the ORR: it involves the reduced form of the complex in which the state of iron oxidation is 2+. This enables interaction between the O_2 molecule and the metal ion to form charge-transfer complex $O_2^- \leftarrow Fe^{III}(ms\text{-}Py)_4P$, which lowers the energy of the chemical bonds in the O_2 molecule and facilitates the four-electron transfer pathway for the reduction.

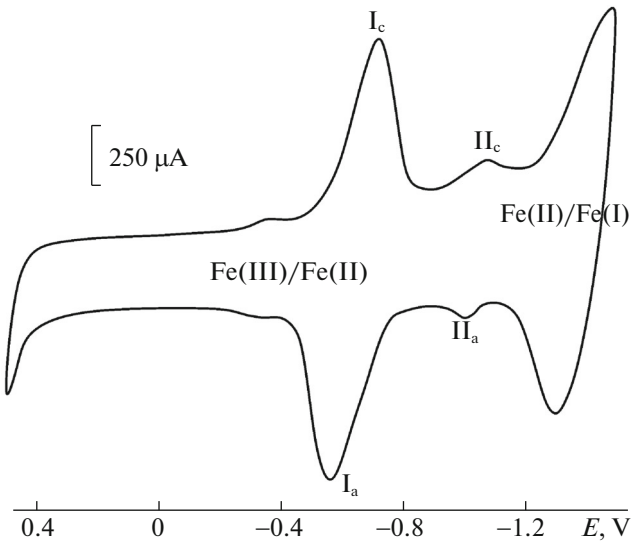

Fig. 3. CVs on the electrode modified with $(Fe(ms\text{-}Ph)_4P)_2O$, at a scan rate of 20 mV s^{-1} under argon.

Of the studied porphyrin complexes, $(FeT(3\text{-}Py)P)_2O$ with the pyridyl nitrogen in the 3-position, displays the highest electrocatalytic activity, which agrees with our earlier results for Co(II) and Cu(II) porphyrins [15]. At the same time, the investigated tetrapyridylporphyrin complexes were somewhat inferior to their Cu(II) and Co(II) counterparts in electrocatalytic activity for the ORR. For cobalt porphyrins $Co^{II}(ms\text{-}(Py\text{-}4)_4)P$ and $Co^{II}(ms\text{-}(Py\text{-}3)_4)P$, $E_{1/2}(O_2)$ = −0.18 and −0.15 V, respectively; for copper porphyrins $Cu^{II}(ms\text{-}(Py\text{-}4)_4)P$ and $Cu^{II}(ms\text{-}(Py\text{-}3)_4)P$, $E_{1/2}(O_2)$ = −0.19 and −0.16 V [15]. This could be due to both the specific properties of the forms of these complexes in alkaline aqueous solutions and the possible irreversible oxidation of the central metal ions, which is fairly common for iron-containing catalysts.

Table 2. Peak potential $E_{max}(O_2)$ and half-wave potential $E_{1/2}(O_2)$ on the porphyrin-modified electrodes

Porphyrin compound	$-E_{max}(O_2)$, V	$-E_{1/2}(O_2)$, V
Without catalyst	0.40	0.30
H_2(*ms*-Ph)$_4$P [17]	0.34	0.28
(Fe(*ms*-Ph)$_4$P)$_2$O	0.34	0.27
H_2(*ms*-Py-4)$_4$P	0.26	0.21
(Fe[*ms*-(Py-4)$_4$]P)$_2$O	0.25	0.25
H_2(*ms*-Py-3)$_4$P	0.23	0.18
(Fe[*ms*-(Py-3)$_4$]P)$_2$O	0.21	0.23
(Fe[*ms*-(Py-3)Ph$_3$]P)$_2$O	0.38	0.28

ACKNOWLEDGMENTS

This work was conducted at the Research Institute of Macroheterocyclic Compounds (Ivanovo State University of Chemistry and Technology). It was supported by RF Presidential Research Grant no. MK-249.2017.3.

REFERENCES

1. K. A. Askarov, B. D. Berezin, and E. V. Bystritskaya, *Porphyrins: Spectroscopy, Electrochemistry, Application* (Nauka, Moscow, 1987) [in Russian].
2. N. Shirley, K. B. F. Gabriel, M. U. Geani, and A. D. F. C. Kelly, Molecules **18**, 7279 (2013).
3. M. R. Tarasevich and K. A. Radyushkina, *Catalysis and Electrocatalysis by Metal Porphyrins* (Nauka, Moscow, 1982) [in Russian].
4. N. Phougat, P. Vasudevan, N. K. Jha, and D. K. Bandhopadhyay, Trans. Met. Chem. **28**, 838 (2003).
5. J. H. Zagal, in *Handbook of Fuel Cells–Fundamentals, Technology and Applications,* Ed. by W. Vielstich, A. Lamm, and H. A. Gasteiger (Wiley, Chichester, 2003), Vol. 2, Ch. 5, p. 544.
6. K. M. Kadish and E. V. Caemelbecke, J. Solid State Electrochem. **7**, 254 (2003).
7. A. Harriman and J.-P. Sauvage, Chem. Soc. Rev. **25**, 41 (1996).
8. B. Sun, Z. Ou, D. Meng, et al., Inorg. Chem. **53**, 8600 (2014).
9. T. N. Lomova, Usp. Khim. Porfir. **3**, 233 (2001).
10. K. M. Kadish, E. V. Caemelbecke, and G. Royal, in *The Porphyrin Handbook,* Ed. by K. M. Kadish (Academic, San Diego. 2000), Vol. 8, Chap. 55, p. 1.
11. K. M. Kadish and E. V. Caemelbecke, Inorg. Chem. **37**, 1759 (1998).
12. P. Bhyrappa, M. Sankar, and B. Varghese, Inorg. Chem. **45**, 4136 (2006).
13. K. M. Kadish, M. Lin, E. V. Caemelbecke, et al., Inorg. Chem. **41**, 6673 (2002).
14. P. Chen, O. S. Finikova, Zh. Ou, et al., Inorg. Chem. **51**, 6200 (2012).
15. N. M. Berezina, M. I. Bazanov, A. S. Semeikin, and A. V. Glazunov, Russ. J. Electrochem. **47**, 42 (2011).
16. A. Brisach-Wittmeyer, S. Lobstein, M. Gross, and A. Giraudeau, J. Electroanal. Chem. **576**, 129 (2005).
17. M. I. Bazanov, N. M. Berezina, D. R. Karimov, and D. B. Berezin, Russ. J. Electrochem. **48**, 905 (2012).
18. Ngoc Minh Do, N. M. Berezina, M. I. Bazanov, et al., Macroheterocycles **8**, 56 (2015).
19. N. M. Do, N. M. Berezina, M. I. Bazanov, et al., J. Porphyr. Phthalocyan. **20**, 615 (2016).
20. D. B. Berezin, *Macrocyclic Effect and Structural Chemistry of Porphyrins* (KRASAND, Moscow, 2010) [in Russian].
21. M. B. Berezin, N. M. Berezina, M. I. Bazanov, A. I. V'yugin, A. S. Semeikin, and A. V. Glazunov, Russ. J. Phys. Chem. A **84**, 1449 (2010).
22. O. V. Samoletov, M. I. Bazanov, A. A. Evseev, et al., Izv. Vyssh. Uchebn. Zaved., Khim. Khim. Tekhnol. **47** (10), 21 (2004).

Translated by A. Kukharuk